A system identification approach to center of mass estimation in trucks

Hamza Benadada, Paolo Massioni, Michaël Di Loreto, Vincent Léchappé, Damien Eberard

A system identification approach to road vehicle center of mass estimation*

Hamza Benadada[1]
Univ. Lyon, INSA Lyon, Université Claude Bernard Lyon 1, Ecole Centrale de Lyon, CNRS, Ampère, UMR5505
69621 Villeurbanne, France
hamza.benadada@insa-lyon.fr

Paolo Massioni[1]
Univ. Lyon, INSA Lyon, Université Claude Bernard Lyon 1, Ecole Centrale de Lyon, CNRS, Ampère, UMR5505
69621 Villeurbanne, France
paolo.massioni@insa-lyon.fr

Michaël Di Loreto[1]
Univ. Lyon, INSA Lyon, Université Claude Bernard Lyon 1, Ecole Centrale de Lyon, CNRS, Ampère, UMR5505
69621 Villeurbanne, France
michael.di-loreto@insa-lyon.fr

Vincent Léchappé[1]
Univ. Lyon, INSA Lyon, Université Claude Bernard Lyon 1, Ecole Centrale de Lyon, CNRS, Ampère, UMR5505
69621 Villeurbanne, France
vincent.lechappe@insa-lyon.fr

Damien Eberard[1]
Univ. Lyon, INSA Lyon, Université Claude Bernard Lyon 1, Ecole Centrale de Lyon, CNRS, Ampère, UMR5505
69621 Villeurbanne, France
damien.eberard@insa-lyon.fr

***Abstract*—The position of the center of mass of a vehicle is an important parameter as it significantly affects vehicle loads distribution and vehicle dynamics. This article proposes an approach to estimate the longitudinal position of the center of mass and the inertial parameters from offline batches. The proposed algorithm is based on the dynamical modelling of the vehicle and on the measurements of cheap gyroscopes and accelerometers. The estimation procedure uses the Box–Jenkins method for system identification to estimate the parameters given the noisy measurements. Prior knowledge of the vehicle is used to filter the output measurement and simplify the estimation problem. The approach is tested on simulations when one or more gyroscopes and accelerometers are used.**

***Index Terms*—System identification, vehicle dynamics, position of the center of mass, measurement noise, Box-Jenkins model.**

I. INTRODUCTION

The wear and tear of the road due to heavy traffic is mainly related to the load on each wheel and each axle of the vehicle rather than to the overall vehicle weight [1] [2]. For this reason, it is of practical interest to estimate such load during the different phases of heavy vehicle operations, considering unloading and distribution routines, even if a weighing scale is not available. It is possible to estimate the load distribution using displacement measurements of the air suspensions [3], but unfortunately not all vehicles feature this kind of suspensions.

Axle loads mainly depend on the total mass of the vehicle and the position of its center of mass. It has been shown that it is possible to estimate accurately the total mass of the vehicle based on inertial measurements such as those provided by gyroscopes and accelerometers [4] [9]. Considering the total mass known, this article aims to introduce a simple procedure to estimate the position of the center of mass. We do not assume the presence of strain sensors or displacement sensors, but only inertial measurements from gyroscopes and accelerometers. In the literature, these measurements are typically fed to a Kalman filter based on a pitch and roll model in order to estimate online the load distribution [3] [5]. In this article, we rely on batch identification instead of Kalman filtering. In fact, the online estimation is useful for estimating time-varying parameters, whereas for this problem the load distribution is mainly related to the center of mass position, which is constant during the vehicle's ride. Batch identification algorithms like the Box-Jenkins methods [6] are less restrictive than online algorithms, as they allow better parameters estimation and better noise filtering [7].

The estimation of the longitudinal and lateral loads distribution can be done using the same approach and modeling. Since the amplitudes of the pitch and roll motions are very small, the coupling effects are often negligible. This article only discusses the estimation of the longitudinal load distribution, but the same approach is applicable for lateral loads. We focus on heavy two-axle vehicles, like a 19 ton truck used for commodities delivery.

II. MODELLING AND PROBLEM FORMULATION

A. Dynamical longitudinal model

The vehicle is modeled by a simple longitudinal planar model, as shown in Fig. 1. The model includes heave and pitch motions of the sprung mass of the vehicle, and the longitudinal displacement of the vehicle [8]. We assume that

*This work was supported by the INSA Lyon VOLVO Industrial Chair.

the vehicle is symmetrical with respect to the vertical plane passing through its longitudinal axis; together with this, we assume that the contact forces and the suspensions are the same for two wheels of the same axle. We also assume that pitch angles, pitch velocity, and pitch acceleration are small.

Considering the longitudinal movement of the vehicle on a plane, according the balance of forces and torques at the center of mass G (see Fig. 1), the motion of the sprung mass can be described as:

$$\begin{aligned} -M_s g + F_1 + F_2 &= M_s \ddot{z}, \\ -F_1 a_1 + F_2 a_2 - M_s \ddot{x} H &= I_{yy} \ddot{\psi}, \end{aligned} \tag{1}$$

where M_s is the sprung mass, I_{yy} the moment of inertia of the sprung mass with respect to the roll axis, F_1 the vertical force applied on the front axle, F_2 the vertical force applied on the rear axle, a_1 the horizontal distance between the front axle and center of mass, a_2 the horizontal distance between the rear axle and the center of mass, H the height of the center of mass, ψ the pitch angle, z the vertical displacement of the sprung mass, and x the longitudinal displacement of the vehicle. Equation (1) leads directly to an explicit expression of the forces F_1 and F_2:

$$\begin{aligned} F_1 &= \tfrac{a_2}{a_1+a_2} M_s g - \tfrac{H}{a_1+a_2} M_s \ddot{x} + \tfrac{a_2}{a_1+a_2} M_s \ddot{z} - \tfrac{I_{yy}}{a_1+a_2} \ddot{\psi}, \\ F_2 &= \tfrac{a_1}{a_1+a_2} M_s g + \tfrac{H}{a_1+a_2} M_s \ddot{x} + \tfrac{a_1}{a_1+a_2} M_s \ddot{z} + \tfrac{I_{yy}}{a_1+a_2} \ddot{\psi}. \end{aligned} \tag{2}$$

The load is composed of static terms and load transfer terms; the static load is $\frac{a_{1,2}}{a_1+a_2} M_s g$ and the load transfer is composed of the other terms. The load transfer is actually very small compared the static one, it often represents at most 5% of total load.

The suspensions are modeled with a parallel spring damper.

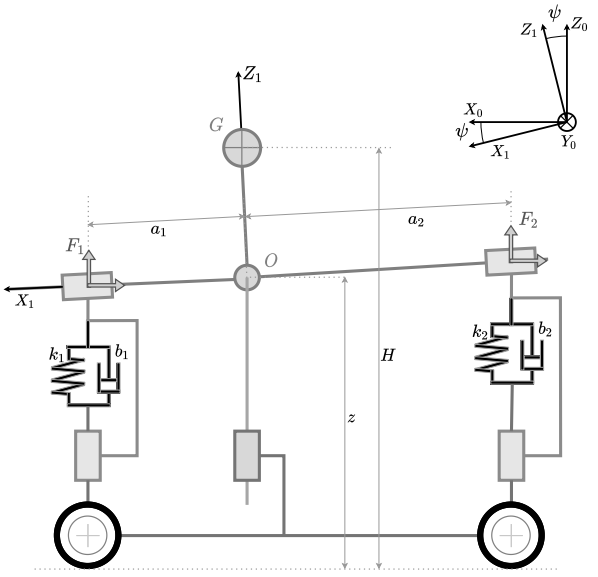

Fig. 1. Longitudinal planar model

The forces F_1 and F_2 can then be expressed as:

$$\begin{aligned} F_1 &= -k_1(z - a_1\psi) - b_1(\dot{z} - a_1\dot{\psi}) + C_1, \\ F_2 &= -k_2(z + a_2\psi) - b_2(\dot{z} + a_2\dot{\psi}) + C_2, \end{aligned} \tag{3}$$

where k_1 is the overall stiffness of the front suspensions, k_2 the overall stiffness of the rear suspensions, b_1 the overall damping of the front suspensions, b_2 the overall damping of the rear suspensions, and C_1 and C_2 are constants that are not relevant for the follow-up.

The unsprung mass and suspensions parameters are usually provided by the vehicle manufacturer, although there may be some uncertainties on the parameters. The sprung mass is assumed to be known since previous works [4] [9] propose efficient approaches to estimate it.

The model resulting from equations (2) and (3) shows a link between the vehicle's longitudinal acceleration and the pitch motion through a number of parameters. These displacements can be measured with gyroscopes and accelerometers. Using an adequate formulation, the modeling and the measurement allow the estimation of the unknown parameters, and then (2) can later be used to estimate the axle loads.

The set of the unknown parameters is noted $\theta = \{a_1, H, I_{yy}\}$. Since the wheelbase $L = a_1 + a_2$ is a known parameter, only a_1 appears in θ.

B. Measurements

We consider two different cases of instrumentation.

Case 1: A gyroscope and an accelerometer measure the longitudinal accelerations $\ddot{x}$ and the angular velocities $\dot{\psi}$ of the vehicle.

Case 2: A couple of gyroscopes and accelerometers are placed each above the two axles. The longitudinal accelerations $\ddot{x}$ and the angular velocities $\dot{\psi}$ measured in the front and rear of the vehicle are the same assuming that the vehicle is a rigid body. Using vertical acceleration measured on the front axle $\ddot{z}_1$ and the one measured on the rear axle $\ddot{z}_2$, we can obtain the angular acceleration $\ddot{\psi}$ as: $\ddot{\psi} = \frac{\ddot{z}_2 - \ddot{z}_1}{L}$. This redundancy allows reducing the measurement noise effects on the estimations.

C. Measurements noises

The gyroscope and accelerometer measurements are noisy [10]. These measurements are usually modeled as:

$$x_m(t) = x(t) + w(t) \quad \text{where: } w(t) = v(t) + b(t),$$

where $x_m(t)$ is the measured signal with a gyroscope or an accelerometer, $x(t)$ the is the real signal, $w(t)$ an additive noise composed of $v(t)$, a white noise, and $b(t)$, a bias. The bias changes over time, but for small time scales it can be considered constant.

D. Transfer functions

Equations (2) and (3) allow the modeling of the pitch and heave motions of a vehicle, the model input is $u = \ddot{x}$ and its outputs are $y_1 = \dot{\psi}$ and $y_2 = \ddot{\psi}$. Let us note $P_1(s)$ the transfer function from u to y_1 and $P_2(s)$ the one from u to

y_2. The second output y_2 is the derivative of the first one y_1, so the transfer function $P_2(s)$ from u to y_2 can be found as $P_2(s) = sP_1(s)$. We can express $P_1(s)$ as:

$$P_1(s) = \frac{-HM_s s(k_1 + k_2 + (b_1 + b_2)s + M_s s^2)}{(k_1 a_1^2 + k_2 a_2^2 + (b_1 a_1^2 + b_2 a_2^2)s + I_{yy} s^2)(k_1 + \ldots + k_2 + (b_1 + b_2)s + M_s s^2) + R} \quad (4)$$

with $R = (a_1 k_1 - a_2 k_2)^2 + ((2a_1 a_2 (k_1 b_2 + k_2 b_1) - (a_1^2 + a_2^2)(k_1 b_1 + k_2 b_2))s - (a_1 b_1 - a_2 b_2)^2 s^2$. This term R is due to the coupling between the pitch motion and the heave motion, and it is equal to zero when there is no coupling effect. It turns out that this term is often negligible. In fact, heave motion is uncomfortable for the passengers and in order to reduce it, the manufacturers usually design the vehicles so that there is no coupling between pitch and heave motions. This appears on the transfer function as two close pairs of poles and zeros.

The identification of a transfer function with close poles and zeros is actually a hard task, especially when the signals are noisy. To have a reliable estimate, the system input signal needs to be rich enough in a very specific frequency band, which is unlikely for our specific application.

E. Simplifying the identification problem

An alternative approach is possible for our problem. For the modeled vehicle, the transfer function zeros depends only on known parameters. These known zeros can be used to filter the output signal, leading to a simpler identification problem.

Let us note $Y_1(s)$ the Laplace transform of the first output, $U(s)$ the Laplace transform of the input, and for notation simplicity let us also note $\text{Den}(s)$ the denominator of the transfer function $P_1(s)$ in equation (4).

The transfer function numerator can be factored with $s(k_1 + k_2 + (b_1 + b_2)s + M_s s^2)$, this term depends only on suspension parameters and the unsprung mass, which are known. Consequently, the input-output relation $Y_1(s) = P_1(s)U(s)$ can be rearranged as:

$$Y_{1f}(s) = T(s)U(s),$$

where $Y_{1f}(s) = F_1(s)Y_1(s)$ is the Laplace transform of the filtered output y_{1f}, $F_1(s) = \dfrac{1}{s(k_1 + k_2 + (b_1 + b_2)s + M_s s^2)}$ is the filter, and $T(s) = \dfrac{-HM_s}{\text{Den}(s)}$ is the transfer function from the input to the filtered output y_{1f}.

The filtered output y_{1f} can easily be computed from the measured output signal. Since the filter is a low-pass one, an additional advantage is the filtering of high-frequency noise on the output signal. The transfer function $T(s)$ is a 4^{th} order transfer function with two pairs of complex conjugate poles, without the close pole-zero couple, which makes its identification simpler.

On the other hand, the second output y_2 is the derivative of the first one y_1. Using the filter $F_2(s) = sF_1(s)$ leads to the same transfer function $T(s)$:

$$Y_{2f}(s) = T(s)U(s),$$

with $Y_{2f}(s)$ the Laplace transform of the filtered output y_{2f}.

The transfer function from the input to the filtered first output and to the filtered second output is the same, so during the identification procedure we can concatenate the signal and estimate the transfer function from both outputs at once.

The second output $y_2 = \ddot{\psi}$ is considered only in case 2 where this signal is measured.

The unknown parameters θ can be obtained either from an estimate of $P_1(s)$ or $P_2(s)$ using directly the measured signals, or from an estimate of $T(s)$ using filtered outputs.

In addition, there are 7 parameters in $P_1(s)$ and $P_2(s)$ (resp. 5 in $T(s)$), whereas there are only 3 unknown parameters $\theta = \{a_1, H, I_{yy}\}$. It is always possible to recover θ from the parameters of $P_1(s)$ and $P_2(s)$ but there is no unique approach.

F. Problem formulation

To conclude this section, let us state again that the goal of this work is to find a reliable estimate of the parameters θ given noisy measurements from gyroscopes and accelerometers.

In order to propose a solution to this problem, we first look into system identification approaches to estimate the transfer functions parameters given noisy measurements, then we analyze the effect of the transfer function simplification and of the measurements redundancy on the parameters estimation.

III. Identification approaches

In this section, we focus on the identification of a discrete-time transfer function in presence of additive noises on the input and the output. The identification algorithms used in this work are based on a discrete-time representation, which is the most common and more natural setting, but the estimated transfer function can subsequently easily be converted to a continuous-time transfer function. For purpose of clarity, we present the identification of systems with only one output, but the same approach holds for multiple outputs.

A. Noise Model

In system identification, it is very important to take into account the noise.In this work, the measurements noises are modeled as additive noises on the input and on each output.

Let $w_1(k)$ be the input noise, the sum of a bias $b_1(k)$ and a white noise $v_1(k)$: $w_1(k) = b_1(k) + v_1(k)$. This relation stands for any value of k, so we can express $w_1(k-1) = b_1(k) + v_1(k-1)$. Since the bias varies slowly, we can assume that $b_1(k) = b_1(k-1)$, which leads to: $w_1(k) = w_1(k-1) + v_1(k) - v_1(k-1)$. Let us set $e_1(k) = v_1(k) - v_1(k-1)$, since $v_1(k)$ is a white noise, $e_1(k)$ is also a white noise.

Overall, the input noise $w_1(k)$ can be modeled as a random walk: $w_1(k) = w_1(k-1) + e_1(k)$. Using the z transform, we can express $w_1(k)$ as:

$$w_1(k) = \frac{z}{z-1} e_1(k).$$

The same reasoning is applied for the output. The measured input u_m and output y_m can be expressed as:

$$u_m(k) = u(k) + \frac{z}{z-1}e_1(k),$$
$$y_m(k) = y(k) + \frac{z}{z-1}e_2(k).$$

B. Model structure

Let $P(z)$ be the transfer function from $u(k)$ to $y(k)$.

Given the noisy measurements $u_m(k)$ and $y_m(k)$, we can represent this model structure as in Fig. 2. The measured

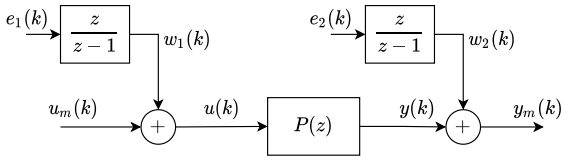

Fig. 2. Model structure with noise

output can be expressed as:

$$y_m(k) = P(z)u_m(k) + \tfrac{z}{z-1}\left(P(z)e_1(k) + e_2(k)\right). \quad (5)$$

The noise term (5) can be represented as:

$$\frac{z}{z-1}\left(P(z)e_1(k) + e_2(k)\right) = G(z)e(k),$$

where $e(k)$ is a white noise and $G(z)$ is a shape filter.

The obtained model is represented in Fig. 3. This model structure correspond to the Box Jenkins (BJ) model [6]. When estimating a BJ model, the noise model $G(z)$ is also estimated, so we only need to correctly guess its order. Since the noise here is the sum of an integrated white noise $\frac{1}{1-z^{-1}}e_2(k)$ and an other integrated white noise passing trough the system $\frac{1}{1-z^{-1}}P(z)e_1(k)$, the order of $G(z)$ can be chosen one order higher than $P(z)$.

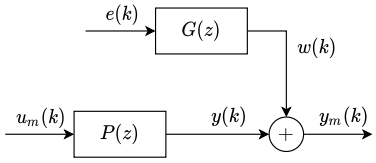

Fig. 3. Box Jenkins model structure

C. Box-Jenkins model estimation and initialization

The Box-Jenkins model is well documented in the literature [6] [7]. The estimation of the model parameters is usually obtained by the minimization of the prediction error, which turns out to be nonlinear and relays on nonlinear numeric optimization routines.

Recently developed algorithms can estimate BJ models with a guaranteed asymptotic global convergence [11], but they might be difficult to implement on a vehicle embedded system. In this work, we will rather use the original algorithm presented by Box and Jenkins in their book [6] with a specific initialization.

The convergence of the BJ algorithm is only guaranteed locally. Hopefully, prior knowledge on the vehicle can be used to initialize the optimization. In fact, for parameters like the position of the center of mass and the pitch inertia moment, any initialization with a coherent order of magnitude turns out to be good enough for the tested cases. For example, the center of mass can be initialized as the geometric center of the vehicle, the pitch inertia moment can be initialized assuming two equal point masses located over each axle.

IV. From estimation to physical parameters

The models identified according to the proposed structures unfortunately do not directly provide the desired physical parameters, but rather the transfer function parameters (either for $P_1(s)$ or $T(s)$). These parameters are nonlinear functions of the vehicle's unknown parameters.

A. From estimation to physical parameters

Let us note p_1, p_2, p_3, p_4, p_5, p_6, and p_7 the parameters of $P_1(s)$, and p the set of these parameters:

$$P_1(s) = \frac{p_5 s + p_6 s^2 + p_7 s^3}{p_1 + p_2 s + p_3 s^2 + p_4 s^3 + s^4}.$$

The parameters p are function of θ, let us note this function $p = f(\theta)$:

$$p_1 = \frac{L^2 k_1 k_2}{I_{yy} M_s},\ p_2 = \frac{L^2(k_1 b_2 + k_2 b_1)}{I_{yy} M_s},$$
$$p_3 = \frac{M_s(a_1^2 k_1 + a_2^2 k_2) + I_{yy}(k_1 + k_2) + L^2 b_1 b_2}{I_{yy} M_s},$$
$$p_4 = \frac{M_s(a_1^2 b_1 + a_2^2 b_2) + I_{yy}(b_1 + b_2)}{I_{yy} M_s}$$
$$p_5 = \frac{-(k_1 + k_2)H}{I_{yy}},\ p_6 = \frac{-(b_1 + b_2)H}{I_{yy}},\ p_7 = \frac{-M_s H}{I_{yy}}.$$

As there are only 3 unknown parameters in θ and 7 in p, there are multiple approaches possible to invert these functions, considering also the presence of estimation errors in the transfer function parameters.

One possibility to recover $\hat{\theta}$ from estimated parameters $\hat{p}$ is to solve the following minimization problem:

$$\hat{\theta} = \arg\min_{\theta} ||\hat{p} - f(\theta)||^2.$$

The solution can be obtained by using a gradient descent algorithm, and it can be initialized by using first estimate obtained from only 3 equations of the form $p = f(\theta)$.

The same approach is used for $T(s)$. Let us note q_1, q_2, q_3, q_4, and q_5 the parameters of $T(s)$, and q the set of theses parameters:

$$T(s) = \frac{q_5}{q_1 + q_2 s + q_3 s^2 + q_4 s^3 + s^4}.$$

The parameters are also functions of θ , let us note this function $q = g(\theta)$ (note that the denominator parameters are the same as for $P_1(s)$):

$$q_1 = p_1, \quad q_2 = p_2, \quad q_3 = p_3, \quad q_4 = p_4, \quad q_5 = \frac{-H}{I_{yy}}.$$

To recover $\hat{\theta}$ from the estimated parameters $\hat{q}$, the same approach as for the first transfer function is used.

V. Main algorithms

The proposed method for the estimate of the position of the center of mass is summarised in the following algorithm:

- Collect the signals $\ddot{x}(t)$, $\dot{\psi}(t)$ (and $\ddot{\psi}$ for case 2);
- set initial guess of the parameters for the estimation;
- estimate the discrete-time Box-Jenkins models;
- convert the estimated models from discrete to continuous-time;
- compute physical parameters θ.

VI. Simulation results

A. Vehicle parameters

The proposed approaches has been tested first on simulations. Data have been generated by using a Matlab model including the pitch motion, the heave motion, the longitudinal displacement, and the coupling between theses motions. The simulated vehicle parameters are listed in Table I. These parameters have been chosen because they lead to relatively less accuracy compared to the other tested ones.

TABLE I
Vehicle parameters

Parameter	Unit	Parameter	Unit
$k_1 = 440000$	N/m	$k_2 = 300000$	N/m
$b_1 = 5000$	kg/s	$b_2 = 12000$	kg/s
$M_s = 15000$	kg	$I_{yy} = 23000$	kg m^2
$a_1 = 1.8$	m	$a_2 = 3.5$	m
$L = 5.3$	m	$H = 1$	m

B. Measurements noises

The measurements noises of gyroscopes and accelerometers have been generated as the sum of a random constant (the bias) and a band-limited white noise. The amplitudes of the biases and the noises spectral densities in the simulations have been chosen as referenced for the MPU-6050 GY-521 sensor module [12], a cheap 6 axes gyroscope and accelerometer sensor unit costing only about 3 euro. For the simulation, the biases for the accelerometers are chosen around ± 0.5 m/s^2 and for the gyroscopes around $20°$/s, and the spectral densities chosen for the accelerometers are 0.004 m/s$^2/\sqrt{\text{Hz}}$, and for the gyroscopes at $0.05°/\text{s}/\sqrt{\text{Hz}}$.

C. Data generation

Since the vehicle simulation and models estimation have short computation times, we run 1000 different simulations. Each simulation lasts 20 s and has a sample time of 0.01 s.

The system input signal is the vehicle acceleration. Input signals are different for each simulation, they have been generated as a succession of ramps and constants with random slopes and amplitudes and with random durations, trying to reproduce the typical cycles of driving along a road. Measurements noises are generated with a Simulink block for band-limited white noise and random biases. The seeds are different for each gyroscope and accelerometers and for each simulation.

Fig. 4 shows an input example, the bold black line is for the real vehicle acceleration and the gray line for the measured one.

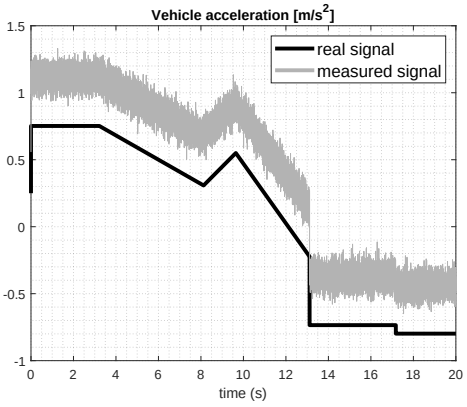

Fig. 4. Vehicle acceleration and measurements noise examples

D. Validation of the estimation methods

The transfer function are estimated using the Box-Jenkins method [6], then the physical parameters $\theta = \{a_1, H, I_{yy}\}$ are recovered according to the methods discussed in Section IV-A. To characterize the quality of the estimation, we look into median values of the estimated parameters (Mdn)[1], their normalized errors (E), and their normalized Root Mean Square Error (RMSE) for the 1000 simulations. Normalized error and normalized RMSE are expressed as percentages and are defined as:

$$\text{E} = \frac{100}{\theta_{real}} \left| \tilde{\theta} - \theta_{real} \right|, \quad \text{RMSE} = \frac{100}{\theta_{real}} \sqrt{\sum_i^n \left(\hat{\theta}_i - \tilde{\theta} \right)^2},$$

where θ_i are the estimated parameter for each simulation, $\tilde{\theta}$ its median, θ_{real} is the real value of the parameters, and n is the number of samples.

Another performance index used is the success rate, that is the number of estimated model with coherent parameter values. The unsuccessful estimations are not considered when computing the performance indexes above.

As discussed in section II-B, Simulation results are presented for two cases of measurement instrumentation.

In the first case, one gyroscope and one accelerometer are used. The available measurements are $\ddot{x}$ and $\dot{\psi}$. Transfer function $P_1(s)$ is estimated directly from the measured signals, and $T(s)$ is estimated after filtering the output signal.

In the second case, two sets of gyroscope and accelerometer units are used. This gives access to two different measures of $\ddot{x}$ and $\dot{\psi}$, and to a measure of $\ddot{\psi}$. This allows estimating also $P_2(s)$, and estimating $T(s)$ after filtering the two output signals.

[1]It is interesting to look into the median values in this work because it corresponds to what one is more likely to get during an estimation.

The estimated parameters obtained from estimation of the different parameters are presented in the box-plot in Fig. 5 and in Table II. In addition, the success rate of the estimation of each transfer function is presented in Table III

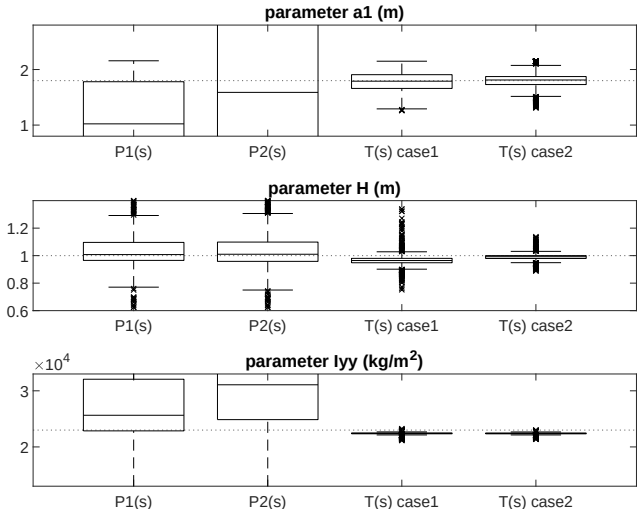

Fig. 5. Estimated parameter boxplot

TABLE II
PARAMETER ESTIMATION FOR CASE 2

	$P_1(s)$			$P_2(s)$		
	Mdn	E(%)	RMSE(%)	Mdn(%)	E(%)	RMSE(%)
$\hat{a}_1$	1.02	43.2	33.9	1.59	11.7	65.9
$\hat{H}$	1.00	0.77	13.2	1.01	1.02	11.1
$\hat{I}_{yy}$	25641	11.5	24.1	31074	35.1	24.2
	$T(s)$ case1			$T(s)$ case2		
	Mdn	E(%)	RMSE(%)	Mdn(%)	E(%)	RMSE(%)
$\hat{a}_1$	1.79	0.55	9.3	1.81	0.63	6.9
$\hat{H}$	0.96	3.55	3.10	0.99	0.78	1.66
$\hat{I}_{yy}$	22429	2.48	0.57	22416	2.54	0.47

TABLE III
TRANSFER FUNCTION ESTIMATION SUCCESS

	$P_1(s)$	$P_2(s)$	$T(s)$ case 1	$T(s)$ case 2
Success rate (%)	61.8	77.2	94.0	97.4

The estimated parameters obtained from a direct identification of $P_1(s)$ or $P_2(s)$ have important deviations and their median values does not necessary correspond the real parameters. In addition, the success rate is somehow disappointing for both transfer function. This might be due to the fact that $P_1(s)$ has two pairs of zeros and poles that are very close. It is actually difficult to identify accurately these close poles and zeros. For the simulated vehicle, $P_1(s)$ has poles for: $p_{1,2} = -2.14 \pm 14.7j$ and $p_{3,4} = -0.594 \pm 6.92j$; its zeros are $z_1 = 0$ and $z_{2,3} = -0.566 \pm 7.00j$.

On the other hand, the estimated parameters obtained from filtering the output and the identification of $T(s)$ have small deviations and the median values close the real parameters (at most 3.5% error). The success rate is close to 100%, with a higher value for the second case. The transfer function $T(s)$ does not have close zeros and poles as the first one, therefore it is simpler to estimate, yielding more accurate results.

When using additional sensors, the estimated parameters have slightly less deviation and more accurate median values for the transfer function $T(s)$. For the case 2, the measurement from different sensors are concatenated in the same identification problem, and since the sensors have different noises, the estimation precision increases.

VII. CONCLUSIONS

This article has illustrated an approach to estimate the position of the center of mass of a road vehicle based on noisy inertial measurements. Unlike previous works based on online algorithms, we have used offline batch identification to estimate the parameters. When using directly the measured signals, the identification does not give reliable estimation of the parameters on simulated data. A solution to this issue has been proposed, consisting in filtering the output and identifying the corresponding transfer function, leading to more precise estimations of the vehicle parameters. Moreover, when using an additional gyroscope and accelerometer, even cheap ones, the estimation quality is improved.

REFERENCES

[1] K. Bayraktarova, L. Eberhardsteiner, C. Aichinger, R. Spielhofer, and R. Blab, "Design life of rigid pavements under dynamic wheel loads," *Road Materials and Pavement Design*, pp. 1–17, 2022.

[2] T. Henning, D. Alabaster, F. Greenslade, A. Fussell, R. Craw *et al.*, "The relationship between vehicle axle loadings and pavement wear on local roads, June 2017," 2017.

[3] M. Doumiati, A. Charara, A. Victorino, and D. Lechner, *Vehicle dynamics estimation using Kalman filtering: experimental validation*. John Wiley & Sons, 2012.

[4] M. N. Mahyuddin, J. Na, G. Herrmann, X. Ren, and P. Barber, "Adaptive observer-based parameter estimation with application to road gradient and vehicle mass estimation," *IEEE Transactions on Industrial Electronics*, vol. 61, no. 6, pp. 2851–2863, 2013.

[5] T. R. Botha and P. S. Els, "Vehicle centre of mass, roll-centre and pitch-centre height estimation," *International Journal of Vehicle Systems Modelling and Testing*, vol. 13, no. 4, pp. 319–339, 2019.

[6] G. E. Box, G. M. Jenkins, G. C. Reinsel, and G. M. Ljung, *Time series analysis: forecasting and control*. Holden-Day, 1970.

[7] L. Ljung, *System identification: Theory for the user*. Prentice Hall, 1987.

[8] J.-P. Brossard, *Dynamique du freinage*. PPUR Presses Polytechniques, 2009.

[9] T. Ersal, I. Kolmanovsky, N. Masoud, N. Ozay, J. Scruggs, R. Vasudevan, and G. Orosz, "Connected and automated road vehicles: state of the art and future challenges," *Vehicle system dynamics*, vol. 58, no. 5, pp. 672–704, 2020.

[10] "IEEE standard specification format guide and test procedure for single-axis laser gyros," *IEEE Std 647-2006 (Revision of IEEE Std 647-1995)*, pp. 1–96, 2006.

[11] Y. Zhu, "A Box-Jenkins method that is asymptotically globally convergent for open loop data," *IFAC Proceedings Volumes*, vol. 44, no. 1, pp. 9047–9051, 2011.

[12] *MPU-6000 and MPU-6050 Product Specification, PS-MPU-6000A-00*, InvenSense Inc., 08 2013, revision 3.4.